*Inorg. Chem.* **2004**, *43*, 2967–2974


# Crystal Structures and Magnetic Properties of Two Low-Dimensional Materials Constructed from $[Mn^{III}(salen)H_2O]^+$ and $[M(CN)_8]^{3-/4-}$ (M = Mo or W) Precursors

**Paweł Przychodzeń,[†] Krzysztof Lewiński,[†] Maria Bałanda,[‡] Robert Pełka,[‡] Michał Rams,[§] Tadeusz Wasiutyński,[‡] Carine Guyard-Duhayon,[||] and Barbara Sieklucka*[,†]**

*Faculty of Chemistry, Jagiellonian University, Ingardena 3, 30-060 Kraków, Poland, H. Niewodniczański Institute of Nuclear Physics PAN, Radzikowskiego 152, 31-342 Kraków, Poland, M. Smoluchowski Institute of Physics, Jagiellonian University, Reymonta 4, 31-059 Kraków, Poland, and Laboratoire de Chimie Inorganique et Matériaux Moléculaires, Unité associée au C. N. R. S. 7071, Université Pierre et Marie Curie, 75252 Paris Cedex 05, France*

Received December 19, 2003

The syntheses, X-ray structures, and magnetic behaviors of two new cyano-bridged assemblies, the molecular $[Mn^{III}(salen)H_2O]_3[W^V(CN)_8]\cdot H_2O$ (**1**) and one-dimensional $[Mn(salen)(H_2O)_2]_2\{[Mn(salen)(H_2O)][Mn(salen)]_2[Mo(CN)_8]\}\cdot 0.5ClO_4\cdot 0.5OH\cdot 4.5H_2O$ (**2**), are presented. Compound **1** crystallizes in the monoclinic system, has space group $P2_1/c$, and has unit cell constants $a = 13.7210(2)$ Å, $b = 20.6840(4)$ Å, $c = 20.6370(2)$ Å, and $Z = 4$. Compound **2** crystallizes in the triclinic system, has space group $P\bar{1}$, and has unit cell dimensions $a = 18.428(4)$ Å, $b = 18.521(3)$ Å, $c = 18.567(4)$ Å, and $Z = 2$. The structure of **1** consists of the asymmetric V-shaped Mn–NC–W–NC–Mn–$O_{phenolate}$–Mn molecules, where W(V) coordinates with $[Mn(salen)H_2O]$ and singly phenolate-bridged $[Mn(salen)H_2O]_2$ moieties through the neighboring cyano bridges. The $[W^V(CN)_8]^{3-}$ ion displays distorted square-antiprism geometry. The structure of **2** consists of the cyano-bridged $\{Mn_3^{III}Mo^{IV}\}_n^-$ repeating units linked by double phenolate bridges into one-dimensional zigzag chains. The Mn(III) centers are bound to Mo(IV) of square-antiprism geometry through the neighboring cyano bridges. The magnetic studies of **1** reveal the antiferromagnetic intramolecular interactions through the CN and phenolate bridges and the relatively weak intermolecular interactions. Compound **1** becomes antiferromagnetically ordered below $T_N = 4.6$ K. The presence of the magnetic anisotropy is documented with the $M(H)$ measurements carried out for both polycrystalline and single-crystal samples. At $T = 1.9$ K, the *spin–flop* transition is observed in the field of 18 kOe applied parallel to the *bc* plane, which is the easy plane of magnetization. Field dependence of magnetization of **1** shows field-induced metamagnetic behavior from the antiferromagnetic ground state of $S_T = {}^3/_2$ to the state of $S_T = {}^5/_2$. The magnetic properties of **2** indicate a weak antiferromagnetic interaction between Mn(III) centers in double-phenolate-bridged $[Mn^{III}(salen)]_2$ dinuclear subunits and a very weak ferromagnetic interaction between them through the diamagnetic $[Mo^{IV}(CN)_8]^{4-}$ spacer.

## Introduction

The formation of supramolecular assemblies based on octacyanometalates $[M(CN)_8]^{3-/4-}$ (M = Mo or W) of potential utility for functional materials is currently attracting much attention.[1,2] The research in this field has resulted in high-nuclearity octacyanometalate based molecules[1] and polymeric coordination networks[2] that behave like magnets and photoinduced magnetic materials.

In the design of new solid state architectures, the strategy of self-assembly through the formation of coordinate M−CN−

* To whom correspondence should be addressed. Phone: +48-12-633-63-77 ext. 2036. E-mail: siekluck@chemia.uj.edu.pl.
[†] Faculty of Chemistry, Jagiellonian University.
[‡] H. Niewodniczański Institute of Nuclear Physics PAN.
[§] M. Smoluchowski Institute of Physics, Jagiellonian University.
[||] Université Pierre et Marie Curie.

(1) (a) Sieklucka, B.; Szklarzewicz, J.; Kemp, T. J.; Errington, W. *Inorg. Chem.* **2000**, *39*, 5156. (b) Bonadio, F.; Gross, M.; Stoeckli-Evans, H.; Decurtins, S. *Inorg. Chem.* **2002**, *41*, 5891. (c) Chang, F.; Sun, H.-L.; Kou, H.-Z.; Gao, S. *Inorg. Chem. Commun.* **2002**, *5*, 660. (d) Arimoto, Y.; Ohkoshi, S.-I.; Zhong, Z. J.; Seino, H.; Mizobe, Y.; Hashimoto, K. *Chem. Lett.* **2002**, *8*, 832−833.

10.1021/ic035464n CCC: $27.50 
Published on Web 04/07/2004

M′ bonds between multidimensional nonrigid octacyanometalates[3] and 3d transition metal tectons, accompanied by weaker $\pi-\pi$ stacking, hydrogen bonding, and electrostatic interactions, has been used.[4] As a part of our program working toward the crystal engineering of magnetic and photomagnetic molecular materials, we are exploring the self-assembly approach for the design of coordination networks involving $(CN)_7M^{IV,V}-CN-Mn^{III}$ linkages.

For the present study, we chose $[Mn^{III}(salen)(H_2O)]^+$ [salen = the N,N′-ethylenebis(salicylideneaminato) dianion], which has a high-spin ground state ($S = 2$), as a building block. The advantage of $[Mn^{III}(salen)(H_2O)]^+$ is the square-planar coordination of the salen ligand that allows the formation of the simplest motifs of both square-pyramidal $[Mn^{III}(salen)(NC)]$ and octahedral $[Mn^{III}(salen)(NC)_2]$ with $[M(CN)_8]^{3-/4-}$ complexes for the construction of multinuclear arrays of low dimensionality.

It has been shown that the reaction of $[Mn^{III}(salen)(H_2O)]^+$ or $[Mn^{III}(BS)]^+$ (BS = the salen-substituted ligand) with $[Fe(CN)_6]^{3-}$ has led to a variety of extended structures, depending on the nature of the Schiff-base ligand, which affects (i) the steric accessibility of $Mn^{III}$ and its coordination number, (ii) the competition of $[Fe(CN)_6]^{3-}$ with solvent molecules at the Mn(III) center, and finally (iii) the equilibrium of the mononuclear $[Mn^{III}(salen)H_2O]^+$ and dinuclear $[Mn^{III}_2(salen)_2(H_2O)_2]^{2+}$ complexes in aqueous solution.[5−10]

Herein we report the syntheses, the crystal structures, and the magnetic properties of two new cyano- and $O_{phenolate}$-bridged compounds: the zero-dimensional (0-D) $[Mn^{III}(salen)(H_2O)]_3[W^V(CN)_8]\cdot H_2O$ tetranuclear molecule (abbreviated as $Mn_3^{III}W^V$ or **1**) and the one-dimensional (1-D) $[Mn^{III}(salen)(H_2O)_2]_2\{[Mn^{III}(salen)(H_2O)][Mn^{III}(salen)]_2[Mo^{IV}(CN)_8]\}\cdot 0.5ClO_4\cdot 0.5OH\cdot 4.5H_2O$ chain (abbreviated as **2**). Both compounds form three-dimensional (3-D) supramolecular networks utilizing $\pi-\pi$ stacking interactions of the salen ligand and hydrogen bonding. The magnetic studies of **1** reveal an antiferromagnetic long-range ordering ($T_N$ = 4.6 K) with planar anisotropy and the *spin−flop* transition in the external magnetic field. Compound **2** is a magnetic chain of weakly coupled double-phenolate-bridged $[Mn^{III}(salen)]_2$ dinuclear subunits separated by the diamagnetic $[Mo^{IV}(CN)_8]^{4-}$ spacer, between which very weak magnetic interactions are observed.

## Experimental Section

**General Procedures and Materials.** All chemicals and solvents were reagent grade. The quadridentate Schiff-base salen ligand ($C_{16}H_{16}N_2O_2$) was prepared by mixing salicylaldehyde and 1,2-diaminoethane in a 2:1 molar ratio in 200 mL of water. The resulting yellow precipitate was recrystallized from ethanol, giving yellow crystals. $K_4[W(CN)_8]\cdot 2H_2O$ and $K_4[Mo(CN)_8]\cdot 2H_2O$ were prepared according to the literature.[11] Since the octacyanometalate ions have a tendency to decompose under irradiation, the syntheses of the manganese(III)−tungsten(V) and manganese(III)−molybdenum(IV) complexes were performed in a dark room and at room temperature.

**Caution:** Perchlorate salts are potentially explosive and should only be handled with care and in small quantities.

**Preparation of $[Mn(salen)(H_2O)]ClO_4$.** The manganese(III) complex was obtained by mixing manganese(III) acetate dihydrate (3.73 mmol, 1.00 g) and salen (3.73 mmol, 1.00 g) in methanol (200 mL) and anhydrous sodium perchlorate (5.64 mmol, 0.69 g) in water (80 mL). After evaporation to 40 mL and cooling, the resulting black crystals were collected by suction filtration. Anal. Calcd for $C_{16}H_{16}N_2O_7ClMn$: C, 43.80; H, 3.68; N, 6.39. Found: C, 44.00; H, 3.71; N, 6.25.


(2) (a) Lu, J.; Harrison, W. T. A.; Jacobson, A. J. *Angew. Chem., Int. Ed.* **1995**, *34*, 2557. (b) Sra, A. K.; Rombaut, G.; Lahitête, F.; Golhen, S.; Ouahab, L.; Mathonière, C.; Yakhmi, J. V.; Kahn, O. *New J. Chem.* **2000**, *24*, 871. (c) Rombaut, G.; Mathonière, C.; Guionneau, P.; Golhen, S.; Ouahab, L.; Verelst, M.; Lecante, P. *Inorg. Chim. Acta* **2001**, *326*, 27. (d) Rombaut, G.; Verelst, M.; Golhen, S.; Ouahab, L.; Mathonière, C.; Kahn, O. *Inorg. Chem.* **2001**, *40*, 1151. (e) Ohkoshi, S.; Hashimoto, K. *J. Photochem. Photobiol., C* **2001**, *2*, 71. (f) Podgajny, R.; Dromzée, Y.; Kruczała, K.; Sieklucka, B. *Polyhedron* **2001**, *20*, 685 (g) Li, D.-F.; Gao, S.; Zheng, L.-M.; Sun, W.-Y.; Okamura, T.; Ueyama, N.; Tang, W.-X. *New J. Chem.* **2002**, *4*, 485. (h) Li, D.-F.; Okamura, T.; Sun, W.-Y.; Ueyama, N.; Tang, W.-X. *Acta Crystallogr.* **2002**, *C58*, m280. (i) Li, D.-F.; Gao, S.; Zheng, L.-M.; Tang, W.-X. *J. Chem. Soc., Dalton Trans.* **2002**, 2805. (j) Sieklucka, B.; Podgajny, R.; Korzeniak, T.; Przychodzeń, P.; Kania, R. *C. R. Chem.* **2002**, *5*, 1. (k) Podgajny, R.; Korzeniak, T.; Bałanda, M.; Wasiutyński, T.; Errington, W.; Kemp, T. J.; Alcock, N. W.; Sieklucka, B. *Chem. Commun.* **2002**, 1138. (l) Szklarzewicz, J.; Podgajny, R.; Lewiński, K.; Sieklucka, B. *CrystEngComm* **2002**, *4* (35), 199. (m) Kania, R.; Lewiński, K.; Sieklucka, B. *J. Chem. Soc., Dalton Trans.* **2003**, 1033. (n) Li, D.-F.; Zheng, L.-M.; Wang, X.-Y.; Huang, J.; Gao, S.; Tang, W.-X. *Chem. Mater.* **2003**, *15*, 2094. (o) Korzeniak, T.; Podgajny, R.; Alcock, N. W.; Lewiński, K.; Bałanda, M.; Wasiutyński, T.; Sieklucka, B. *Polyhedron* **2003**, *22*, 2183. (p) Podgajny, R.; Desplanches, C.; Fabrizi de Biani, F.; Sieklucka, B.; Dromzée, Y.; Verdaguer, M. To be submitted for publication. (q) Podgajny, R.; Korzeniak, T.; Stadnicka, K.; Dromzée, Y.; Alcock, N. W.; Errington, W.; Kruczała, K.; Bałanda, M.; Kemp, T. J.; Verdaguer, M.; Sieklucka, B. *J. Chem. Soc., Dalton Trans.* **2003**, 3458. (r) Herrera, J. M.; Armentano, D.; de Munno, G.; Lloret, F.; Julve, M.; Verdaguer, M. *New J. Chem.* **2003**, *27*, 128. (s) Chen, F.-T.; Li, D.-F.; Gao, S.; Wang, X.-Y.; Zheng, L.-M.; Tang, W.-X. *J. Chem. Soc., Dalton Trans.* **2003**, 3283. (t) Larionova, J.; Clérac, R.; Donnadieu, B.; Willemin, S.; Guérin C. *Cryst. Growth Des.* **2003**, *3*, 267. (u) Arimoto, Y.; Ohkoshi, S.-I.; Zhong, Z. J.; Seino, H.; Mizobe, Y.; Hashimoto, K. *J. Am. Chem. Soc.* **2003**, *125*, 9240. (v) Li, D.-F.; Zheng, L.; Zhang, Y.; Huang, J.; Gao, S.; Tang, W. *Inorg. Chem.* **2003**, *42*, 6123. (w) Herrera, J. M.; Bleuzen, A.; Dromzée, Y.; Julve, M.; Lloret, F.; Verdaguer, M. *Inorg. Chem.* **2003**, *42*, 7052.

(3) (a) Muetterties, E. L. *Inorg. Chem.* **1973**, *12*, 1963. (b) Burdett, J. K.; Hoffmann, R.; Fay, R. C. *Inorg. Chem.* **1978**, *17*, 2553. (c) Leipoldt, J. G.; Basson, S. S.; Roodt, A. *Adv. Inorg. Chem.* **1993**, *40*, 241. (d) Leipoldt, J. G.; Basson, S. S.; Roodt, A.; Purcell, W. *Polyhedron* **1992**, *11*, 2277.

(4) (a) Batten, S. R.; Robson, R. *Angew. Chem., Int. Ed.* **1998**, *37*, 1460. (b) Zaworotko, M. J. *Chem. Commun.* **2001**, 1. (c) Holliday, B. J.; Mirkin, Ch. A. *Angew. Chem., Int. Ed.* **2001**, *40*, 2022. (d) Moulton, B.; Zaworotko, M. J. *Chem. Rev.* **2001**, *101*, 1629. (e) Batten, S. R. *Solid State Mater.* **2001**, *5*, 107. (f) Batten, S. R. *CrystEngComm* **2001**, *18*, 1. (g) Hunter, Ch. A.; Sanders, J. K. M. *J. Am. Chem. Soc.* **1990**, *112*, 5525. (h) Krass, H.; Plummer, E. A.; Heider, J. M.; Barker, Ph. R.; Alcock, N. W.; Pikramenou, Z.; Hannon, M. J.; Kurth, D. G. *Angew. Chem., Int. Ed.* **2001**, *40*, 3862. (i) Lu, J.; Mondal, A.; Moulton, B.; Zaworotko, M. J. *Angew. Chem., Int. Ed.* **2001**, *40*, 2113. (j) Nichols, P. J.; Raston, C. L.; Steed, J. W. *Chem. Commun.* **2001**, 1062. (k) Steed, J. W.; Atwood, J. L. *Supramolecular Chemistry*; J. Wiley & Sons: Chichester, U.K., 2000; pp 19−30, 390−392.

(5) Miyasaka, H.; Okawa, H.; Miyazaki, A.; Enoki, T. *J. Chem. Soc., Dalton Trans.* **1998**, 3991.

(6) Miyasaka, H.; Ieda, H.; Matsumoto, N.; Re, N.; Crescenzi, R.; Floriani, C. *Inorg. Chem.* **1998**, *37*, 255.

(7) Miyasaka, H.; Matsumoto, N.; Re, N.; Gallo, E.; Floriani, C. *Inorg. Chem.* **1997**, *36*, 670.

(8) Miyasaka, H.; Matsumoto, N.; Okawa, H.; Re, N.; Gallo, E.; Floriani, C. *J. Am. Chem. Soc.* **1996**, *118*, 981.

(9) Re, N.; Gallo, E.; Floriani, C.; Miyasaka, H.; Matsumoto, N. *Inorg. Chem.* **1996**, *35*, 6004.

(10) Miyasaka, H.; Matsumoto, N.; Okawa, H.; Re, N.; Gallo, E.; Floriani, C. *Angew. Chem., Int. Ed. Engl.* **1995**, *34*, 1446.

(11) Leipoldt, J. G.; Bok, L. C. D.; Cilliers, P. J. *Z. Anorg. Allg. Chem.* **1974**, *409*, 343.

**Preparation of $[Mn(salen)(H_2O)]_3[W(CN)_8]\cdot H_2O$ (1).** To a solution of $[Mn(salen)H_2O]ClO_4$ (0.23 mmol, 0.10 g) in water (25 mL), a solution of $K_4[W(CN)_8]\cdot 2H_2O$ (0.23 mmol, 0.13 g) in water (10 mL) was added. The reaction mixture was stirred for 10 min and then filtered. Dark-brown crystals of **1** suitable for X-ray single-crystal structure determination were obtained by slow evaporation of the filtrate in the dark at room temperature for 5 weeks. The crystals were collected by suction filtration, washed with water, and air-dried. Yield: 92.5 mg, 29%. Anal. Calcd for $C_{56}H_{50}N_{14}O_{10}Mn_3W$: C, 47.11; H, 3.53; N, 13.73. Found: C, 47.36; H, 3.48; N, 13.44. IR (KBr): $\nu$(CN) 2138, 2150, 2157, 2165 $cm^{-1}$.

**Preparation of $[Mn(salen)(H_2O)_2]_2\{[Mn(salen)(H_2O)][Mn(salen)]_2[Mo(CN)_8]\}\cdot 0.5ClO_4\cdot 0.5OH\cdot 8H_2O$ ($2\cdot 3.5H_2O$).** To a solution of $[Mn(salen)H_2O]ClO_4$ (0.23 mmol, 0.10 g) in water (20 mL), a solution of $K_4[Mo(CN)_8]\cdot 2H_2O$ (0.23 mmol, 0.11 g) in water (10 mL) was added. The reaction mixture was stirred for 20 min and then filtered, and the filtrate was left at room temperature in the dark room for evaporation. After one week, the dark-brown precipitate was collected by suction filtration, washed with water, and air-dried. Yield: 32.7 mg, 7%. Anal. Calcd for $C_{88}H_{96.5}N_{18}O_{25.5}Mn_5MoCl_{0.5}$ ($2\cdot 3.5H_2O$): C, 47.98; H, 4.42; N, 11.45. Found: C, 47.58; H, 4.21; N, 11.56. IR (KBr): $\nu$(CN) 2103 $cm^{-1}$. Dark-brown crystals of **2** were grown by very slow evaporation of the filtrate in the dark at room temperature for 4 weeks. The crystals were collected by suction filtration, washed with water, and air-dried.

**Physical Measurements.** Infrared spectra were measured between 4000 and 400 $cm^{-1}$ on a Bruker EQUINOX 55 spectrometer in KBr disks. Magnetic susceptibility measurements were performed upon cooling in a constant magnetic field of 2 kOe over the temperature range 1.9−300 K using a Quantum Design SQUID magnetometer. Isothermal magnetization curves in the field up to 50 kOe were measured at $T = 1.9$ and 4.3 K. Magnetic studies have been carried out for powder and single-crystal samples of **1**. The single-crystal sample (approximate size, $0.2 \times 0.6 \times 0.8$ $mm^3$) was oriented by the X-ray analysis. Experimental data were corrected for diamagnetic ($\chi_{dia}$) and temperature-independent-paramagnetic ($\chi_{TIP}$) contributions.

**X-ray Data Collection and Structure Determination.** Single-crystal X-ray data for $[Mn^{III}(salen)(H_2O)]_3[W^V(CN)_8]\cdot H_2O$ (**1**) and $[Mn^{III}(salen)(H_2O)_2]_2\{[Mn^{III}(salen)(H_2O)][Mn^{III}(salen)]_2[Mo^{IV}(CN)_8]\}\cdot 0.5ClO_4\cdot 0.5OH\cdot 4.5H_2O$ (**2**) were collected at room temperature on a Nonius KappaCCD diffractometer with graphite monochromated Mo K$\alpha$ radiation ($\lambda = 0.7107$ Å). For compound **1**, the Denzo Scalepack program package was used for cell refinement and data reduction.[12] The multiscan absorption correction based on equivalent reflections was applied to the data. The structure of **1** was solved by the heavy atom method (SHELXS-97) and subsequent Fourier analyses and refined by full-matrix least-squares on $F^2$ using the program SHELXL-97.[13] Anisotropic displacement parameters were applied to all non-hydrogen atoms. The hydrogen atoms of the salen molecules were located in their calculated positions and refined using a riding model with individual isotropic displacement parameters. In all the water molecules, the hydrogens were localized on difference Fourier maps and refined with individual isotropic displacement parameters. The restraints were applied to O4 to hydrogen distances of the crystalline water molecule. The diffraction data of compound **2** were reduced using the EvalCCD program package.[14] The structure of **2** was solved by direct methods and subsequent difference Fourier syntheses and refined by full-matrix least-squares on $F$ using the programs of the PC version of CRYSTALS.[15] All non-$H_2O$ and -$ClO_4$ molecules and non-hydrogen atoms were refined anisotropically. Hydrogen atoms were introduced in calculated positions, and only one overall isotropic displacement parameter was refined. The Cl atom of the perchlorate group was located on an inversion center. Complete crystallographic data and collection parameters for both structures are listed in Table 1.

**Table 1.** Summary of Crystal, Intensity Collection, and Refinement Data for $[Mn^{III}(salen)(H_2O)]_3[W^V(CN)_8]\cdot H_2O$ (**1**) and $[Mn^{III}(salen)(H_2O)_2]_2\{[Mn^{III}(salen)(H_2O)][Mn^{III}(salen)]_2[Mo^{IV}(CN)_8]\}\cdot 0.5ClO_4\cdot 0.5OH\cdot 4.5H_2O$ (**2**)

| | **1** | **2** |
|---|---|---|
| empirical formula | $C_{56}H_{50}N_{14}O_{10}Mn_3W$ | $C_{88}H_{89.5}N_{18}O_{22}Mn_5MoCl_{0.5}$ |
| fw | 1427.87 | 2139.82 |
| $\lambda$(Mo K$\alpha$) | 0.7107 | 0.7107 |
| cryst syst | monoclinic | triclinic |
| space group | $P2_1/c$ | $P\bar{1}$ |
| $a$ (Å) | 13.7210(2) | 18.428(4) |
| $b$ (Å) | 20.6840(4) | 18.521(3) |
| $c$ (Å) | 20.6370(2) | 18.567(4) |
| $\alpha$ (deg) | 90 | 94.79(2) |
| $\beta$ (deg) | 102.1290(10) | 119.23(1) |
| $\gamma$ (deg) | 90 | 107.861(16) |
| $V$ (Å$^3$) | 5726.14(15) | 5051.1(21) |
| $\rho_{calc}$ (g $cm^{-3}$) | 1.656 | 1.389 |
| $Z$ | 4 | 2 |
| $\mu$ ($mm^{-1}$) | 2.720 | 0.814 |
| $T$ (K) | 293(2) | 295 |
| reflns/unique | 20 244/12 388 | 22 105/22 105 |
| $R$ indices[a] | $R = 0.0293$[b] | $R = 0.0865$[b] |
| | wR2 = 0.0641[c] | wR = 0.0977[d] |
| $R$ indices (all data) | $R = 0.0438$[b] | $R = 0.1452$[b] |
| | wR2 = 0.0711[c] | wR = 0.1520[d] |
| GOF | 1.022 | 1.076 |

[a] **1**: 10 054 reflections, $I > 2\sigma(I)$; **2**: 12 797 reflections, $I > 3\sigma(I)$. [b] $R = \sum||F_o| - |F_c||/\sum|F_o|$. [c] $wR2 = \{\sum[w(F_o^2 - F_c^2)^2]/\sum[w(F_o^2)^2]\}^{1/2}$. [d] $wR = \{\sum[w(F_o - F_c)^2]/\sum[w(F_o)^2]\}^{1/2}$.

## Results and Discussion

**Formation and General Properties.** $[Mn^{III}(salen)(H_2O)]_3[W^V(CN)_8]\cdot H_2O$ (**1**) was synthesized in water by the reaction of $[Mn^{III}(salen)H_2O]ClO_4$ with $K_4[W^{IV}(CN)_8]\cdot 2H_2O$ in a 1:1 Mn/W molar ratio. Regardless of the Mn/W molar ratio and the $[W^{IV}(CN)_8]^{4-}$ or $[W^V(CN)_8]^{3-}$ complex used, the resulting complex **1** presents a 3:1 stoichiometry and a $W^V$ center. The redox behavior of the $Mn^{III}-W^{IV}$ reaction system can be rationalized in terms of the oxidation of $[W^{IV}(CN)_8]^{4-}$ by $[Mn^{III}(salen)H_2O]^+$, leading to the formation of $[W^V(CN)_8]^{3-}$, and followed by the aerial oxidation of the $[Mn^{II}(salen)H_2O]$ product to $[Mn^{III}(salen)H_2O]^+$.[16] $[Mn(salen)(H_2O)_2]_2\{[Mn(salen)(H_2O)][Mn(salen)]_2[Mo(CN)_8]\}\cdot 0.5ClO_4\cdot 0.5OH\cdot 4.5H_2O$ (**2**) was synthesized in water by the reaction of $[Mn^{III}(salen)H_2O]ClO_4$ with $K_4[Mo^{IV}(CN)_8]\cdot 2H_2O$ in a 1:1 Mn/Mo molar ratio. Complex **2** presents a 5:1 stoichiometry and the original $Mo^{IV}$ center due to the much higher redox potential of the $[Mo(CN)_8]^{3-/4-}$ couple compared with $[W(CN)_8]^{3-/4-}$.[17]

(12) Otwinowski, Z.; Minor, W. *Methods Enzymol*. **1997**, *276*, 307.
(13) Sheldrick, G. M. *SHELX-97*; programs for structure analysis; University of Göttingen: Germany, 1998.
(14) Duisenberg, A. J. M.; Kroon-Batenburg, L. M. J.; Schreurs, A. M. M. *J. Appl. Crystallogr*. **2003**, 220−229.
(15) Watkin, D. J.; Prout, C. K.; Carruthers, J. R.; Betteridge, P. W.; Cooper, R. I. *CRYSTALS*, Issue 11; Chemical Crystallography Laboratory: Oxford, U.K., 2001.
(16) Bermejo, M. R.; Castiñeiras, A.; Garcia-Monteagudo, J. C.; Rey, M.; Sousa, A.; Watkinson, M.; McAuliffe, C. A.; Pritchard, R. G.; Beddoes, R. L. *J. Chem. Soc., Dalton Trans.* **1996**, 2935.
(17) Sieklucka, B. *Prog. React. Kinet.* **1989**, *15*, 175.

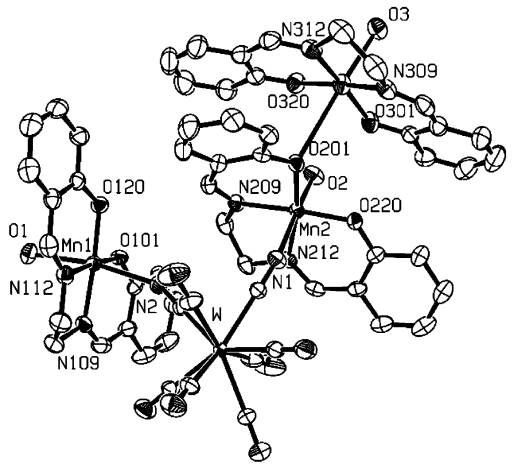


**Figure 1.** Asymmetric unit of **1**.

The $Mn^{III}_3W^V$ molecule (**1**) consists of cyano and single $O_{phenolate}$ bridges with Mn−NC−W−CN−Mn−$O_{phenolate}$−Mn skeletons. Compound **2** consists of cyano-bridged $\{Mn^{III}_3Mo^{IV}\}_n^-$ units linked by double phenolate bridges into infinite zigzag chains. The presence of cyano and phenolate bridges indicates that mononuclear $[Mn^{III}(salen)H_2O]^+$ and dinuclear $[Mn^{III}_2(salen)_2(H_2O)_2]^{2+}$ forms are engaged in the self-assembly process of **1** and **2**, in agreement with the equilibrium of the forms in aqueous solution.

IR data of $[Mn^{III}(salen)(H_2O)]_3[W^V(CN)_8]\cdot H_2O$ (**1**) revealed four $\nu$(CN) vibrations at 2138 (m), 2150 (s), 2157 (s), and 2165 (m) $cm^{-1}$. The $\nu$(CN) bands of **1** are in the range of those of the isolated octacyanotungstate(V) ion (2170−2130 $cm^{-1}$).[2q,18] This demonstrates that the kinematic coupling [increasing of $\nu$(CN)] in **1** is compensated by the electronic effect. The latter consists of electron withdrawal by [Mn(salen)($H_2O$)] units, which causes enhanced $\pi$-back-donation from the W center to the $\pi$* MOs of cyanide with consequences opposite to those of kinematic coupling. The IR spectrum of $[Mn^{III}(salen)(H_2O)_2]_2\{[Mn^{III}(salen)(H_2O)][Mn^{III}(salen)]_2[Mo^{IV}(CN)_8]\}\cdot 0.5ClO_4\cdot 0.5OH\cdot 4.5H_2O$ (**2**) shows only one broad $\nu$(CN) vibration at 2103 (s) $cm^{-1}$. Taking into account the range 2140−2100 $cm^{-1}$ and the pattern of the $\nu$(CN) bands of the isolated octacyanomolybdate(IV) anion, it is not possible to distinguish between the terminal and bridging $\nu$(CN) bands of **2**.[2q,18]

**Structural Description.** The molecular structure of $[Mn^{III}(salen)(H_2O)]_3[W^V(CN)_8]\cdot H_2O$ (**1**) consists of neutral $[Mn^{III}(salen)(H_2O)]_3[W^V(CN)_8]$ molecules in which linked metallic $Mn^{III}$−NC−$W^V$−CN−$Mn^{III}$−$O_{phenolate}$−$Mn^{III}$ centers form slightly distorted V-shaped units (Figure 1). The distorted hexacoordinated $[Mn^{III}(salen)(H_2O)(NC)]$ moieties consist of an equatorial salen ligand, an axial aqua ligand, and, in Mn(1) and Mn(2) centers, nitrogen bonded cyanides bridging Mn(III) to the W(V) center. Relevant bond distances and angles are listed in Table 2 and Supporting Information Table S1. The axial positions of the Mn(3) ion are occupied by the phenolate oxygen atom O(201) of the neighboring complex and by a water molecule. The distance of Mn(3) to O(201) equal to 2.979(3) Å is in the middle of the range between short and long distances observed in dinuclear complexes of quadridentate Mn(III) Schiff-base complexes.[19]

The $[W^V(CN)_8]^{3-}$ unit displays a slightly distorted square-antiprism geometry ($D_{4d}$). It has two bridging and six terminal cyano ligands. There is no important difference between the mean values for bridging and terminal cyano ligands, within experimental error. The W−C−N bridging units appear as almost linear in opposition to the case of the strongly bent Mn−N−C units (153.2(3)° and 149.3(3)° for Mn(1)−N(2)−C(2) and Mn(2)−N(1)−C(1), respectively), typical for the cyano-bridged octacyanometalates.

The hydrogen bonds (2.996 Å) between the aqua ligand and the phenolate oxygen as well as the face-to-face $\pi-\pi$ contacts of about 3.3 Å of the salen rings of Mn(1) moieties provide the linking of neighboring $Mn_3^{III}W^V$ molecules (Supporting Information Figure S1). In the crystal, the molecules are arranged in infinite columns along the *a* direction (Figure 2) and stabilized by the well-defined hydrogen bond network (Supporting Information Table S2). The intermolecular intermetallic metal···metal distances are relatively small, being 5.036, 8.536, 7.812, and 4.225 Å for Mn(1)−Mn(1), Mn(2)−Mn(2), Mn(1)−Mn(3), and Mn(2)−Mn(3), respectively.

The crystal structure of $[Mn^{III}(salen)(H_2O)_2]_2\{[Mn^{III}(salen)(H_2O)][Mn^{III}(salen)]_2[Mo^{IV}(CN)_8]\}\cdot 0.5ClO_4\cdot 0.5OH\cdot 4.5H_2O$ (**2**) consists of the anionic $\{[Mn^{III}(salen)(H_2O)][Mn^{III}(salen)]_2[Mo^{IV}(CN)_8]\}_n^-$ 1-D chains, isolated $[Mn^{III}(salen)(H_2O)_2]^+$ and perchlorate counterions, and the water molecules. In the repeating anionic fragment $\{Mn_3Mo\}_n^-$, three Mn(III) moieties of octahedral geometry are coordinated to the neighboring $CN^-$ ligands from the $[Mo^{IV}(CN)_8]^{4-}$ unit of square-antiprism geometry (Figure 3). As in **1**, the cyano bridge and the aqua ligand are arranged in the trans position. Relevant bond distances and angles are listed in Table 3 and Supporting Information Table S3. The Mo−C−N bridging units are almost linear in contrast to the case of the strongly bent Mn−N−C units (150.2, 152.0, and 142.7° for Mn(1)−N(1)−C(1), Mn(2)−N(2)−C(2), and Mn(3)−N(3)−C(3), respectively). The link between the $\{Mn_3Mo\}_n^-$ units is established by the phenolate bridges $[\{Mn(NC)(salen)\}(\mu\text{-}O_{phenolate})_2\{Mn(NC)(salen)\}]$ at the [Mn(1) or Mn(3)] centers (Figure 4). The $\{[Mn^{III}(salen)(H_2O)][Mn^{III}(salen)]_2[Mo^{IV}(CN)_8]\}_n^-$ anions are arranged in infinite zigzag chains along the *b* direction (Figure 5). In the Mn(2) moiety, the sixth axial position is occupied by an aqua ligand, preventing this unit from phenolate bridging. The hydrogen bonds (2.988 Å) between the aqua ligand and the phenolate oxygen as well as face-to-face $\pi-\pi$ contacts of about 3.5 Å of the salen rings of Mn(2) moieties (Supporting Information Figure S2) provide the linking of neighboring chains into layers parallel to the $(10\bar{1})$ plane (Figure 5). The Mn(4) units are connected with each other through aqua ligand and phenolate oxygen hydrogen bonds. The $[Mn(5)(salen)(H_2O)_2]^+$ ions link the two layers by hydrogen bonds between axial aqua ligands and $[Mo^{IV}(CN)_8]^{4-}$ units. The space between the layers is

(18) Griffith, W. P. *J. Chem. Soc., Dalton Trans.* **1975**, 2489.

(19) Miyasaka, H.; Clerac, R.; Ishii, T.; Chang, H.-Ch.; Kitagawa, S.; Yamashita, M. *J. Chem. Soc., Dalton Trans.* **2002**, 1528.

**Table 2.** Relevant Bond Distances (Å) and Angles (deg) for **1** with Estimated Standard Deviations in Parentheses

| $[W(CN)_8]^{3-}$ | | $[Mn(1)(salen)(NC)(H_2O)]^+$ | |
|---|---|---|---|
| W−C range/W−$C_{av}$ | 2.159(4)−2.175(3)/2.166(5) | Mn−N(2) | 2.336(3) |
| C−N range/C−$N_{av}$ | 1.137(5)−1.143(4)/1.141(2) | Mn−N(2)−C(2) | 153.2(3) |
| $[Mn(2)(salen)(NC)(H_2O)]^+$ | | $[Mn(3)(salen)(O_{phenolate})(H_2O)]^+$ | |
| Mn−N(1) | 2.398(3) | Mn−$O_{phenolate}$(201) | 2.979(3) |
| Mn−N(1)−C(1) | 149.3(3) | Mn−$O_{phenolate}$(201)−Mn(2) | 118.4 |

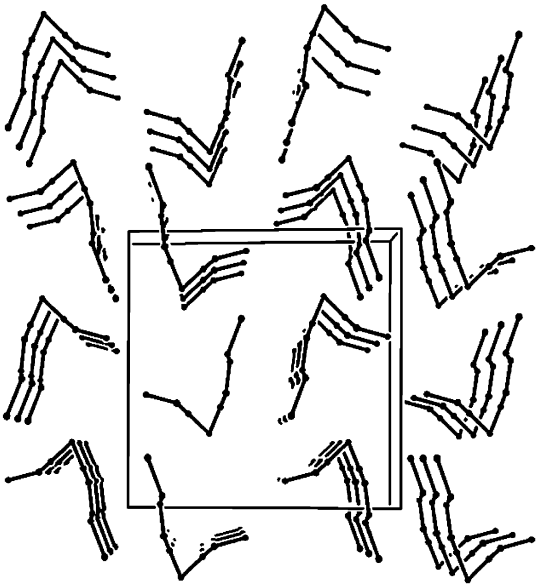

**Figure 2.** Packing diagram of **1** along the *a* axis.

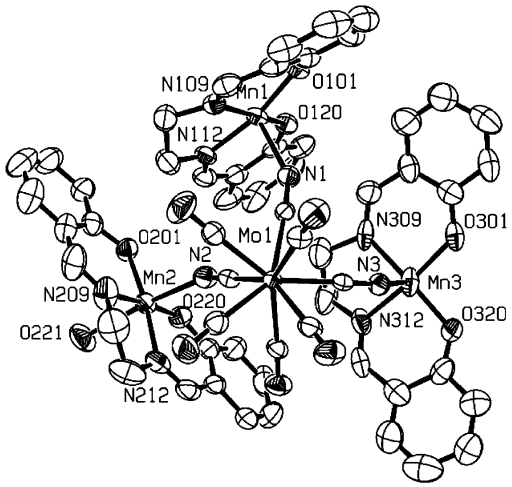


**Figure 3.** Asymmetric unit of **2**.

occupied by $[Mn^{III}(salen)(H_2O)_2]^+$, $ClO_4^-$ ions, and $H_2O$ molecules connected through the hydrogen bond network (Supporting Information Figure S3 with the detailed description).

**Magnetic Properties of a Polycrystalline Sample of 1.** Variable-temperature (1.9−300 K) magnetic susceptibility data were collected on a polycrystalline sample of $[Mn^{III}(salen)(H_2O)]_3[W^V(CN)_8]\cdot H_2O$ (**1**) (Figure 6). The negative Curie−Weiss constant $\Theta = -20$ K (20−300 K) and the low value of $\chi_M$ (0.40 $cm^3\ mol^{-1}$) at the maximum of the $\chi_M$ curve at $T = 4.6$ K indicate the antiferromagnetic coupling in **1** with $T_N = 4.6$ K and a long-range antiferromagnetic ordering. The value $\chi_M T = 8.97\ cm^3\ K\ mol^{-1}$ (8.47 $\mu_B$) at 300 K is in good agreement with the expected value 9.38 $cm^3\ K\ mol^{-1}$ (8.66 $\mu_B$) for three isolated high-spin Mn(III) ions ($S = {}^4/_2$) and one W(V) ion ($S = {}^1/_2$), with $g = 2.00$. As the temperature is lowered, the $\chi_M T$ product continuously decreases, which points to an antiferromagnetic character of the intra- and intermolecular interactions in the system.

According to the X-ray structure, **1** consists of the tetranuclear $Mn^{III}$−NC−$W^V$−CN−$Mn^{III}$−$O_{phenolate}$−$Mn^{III}$ molecules with relatively short intermolecular distances. We have analyzed the data assuming: (i) an isotropic Heisenberg interaction through the CN bridges ($J_1$), (ii) an isotropic coupling of the Mn(III) centers through the phenolate oxygen atom ($J_2$), and (iii) a relatively weak interaction between tetranuclear molecules ($J'$). The calculation of all coupling constants was performed within the framework of molecular field theory.[20] The corresponding phenomenological Hamiltonian has the following form:

$$\mathbf{H} = -J_1(\mathbf{S}_{Mn1}\mathbf{S}_W + \mathbf{S}_W\mathbf{S}_{Mn2}) - J_2\mathbf{S}_{Mn2}\mathbf{S}_{Mn3} + \beta g H\mathbf{S}_{Tz} - zJ'\langle\mathbf{S}_{Tz}\rangle\mathbf{S}_{Tz}$$

where the magnetic field ($H$) is assumed to be along the $z$ direction, $\mathbf{S}_T$ is the total spin operator of the tetramer, with $\mathbf{S}_T = \mathbf{S}_{Mn1} + \mathbf{S}_W + \mathbf{S}_{Mn2} + \mathbf{S}_{Mn3}$, $\mathbf{S}_{Tz}$ is the $z$ component of the $\mathbf{S}_T$ operator, $g$ is the effective Landé factor, and $z$ is the number of the nearest neighbors of the molecule of **1** in the crystal lattice. The magnetic susceptibility in the form of $\chi_M T$ is given by the following formula:

$$\chi_M T = \chi_{mol} T/(1 - \chi_{mol} zJ'/Ng^2\beta^2)$$

where $\chi_{mol}$ denotes the magnetic susceptibility of the isolated tetrameric units. To obtain $\chi_{mol}$ for a fixed set of parameters, the energies of all the spin levels of the tetramer were calculated using standard numerical diagonalization procedures. It is noteworthy that the numerical approach enabled us to take into account a nonzero external magnetic field of $H = 2$ kOe present during the measurements. The best agreement with the experimental data was obtained for $J_1 = -1.5\ cm^{-1}$, $J_2 = -3.9\ cm^{-1}$, $J' = -0.7\ cm^{-1}$, and $g = 1.99$. This set of parameters accurately reproduces all the features of the $\chi_M T$ product over the entire temperature range.

In terms of an intuitive picture, we can conclude that in the $Mn^{III}$−NC−$W^V$−CN−$Mn^{III}$−$O_{phenolate}$−$Mn^{III}$ molecule the relatively strong antiferromagnetic coupling through the phenolate oxygen results in the zero-spin state of the $Mn^{III}$−$O_{phenolate}$−$Mn^{III}$ subunit, whereas the antiferromagnetic in-

(20) Kahn, O. *Molecular Magnetism*; VCH: New York, 1993; pp 26−28.

**Table 3.** Relevant Bond Distances (Å) and Angles (deg) for **2** with Estimated Standard Deviations in Parentheses

| $[Mo(CN)_8]^{4-}$ | | $[Mn(1)(salen)(NC)(O_{phenolate})]^{+}$ | |
|---|---|---|---|
| Mo−C range/Mo−$C_{av}$ | 2.128(8)−2.181(7)/2.155(16) | Mn−N(1) | 2.227(6) |
| C−N range/C−$N_{av}$ | 1.141(9)−1.160(1)/1.152(7) | Mn−N(1)−C(1) | 150.2(5) |
| | | Mn−$O_{phenolate}$(101) | 2.590 |
| | | Mn−$O_{phenolate}$(101)−Mn′ | 99.2 |
| $[Mn(2)(salen)(NC)(H_2O)]^{+}$ | | $[Mn(3)(salen)(NC)(O_{phenolate})]^{+}$ | |
| Mn−N(2) | 2.314(6) | Mn−N(3) | 2.197(6) |
| Mn−N(2)−C(2) | 152.0(6) | Mn−N(3)−C(3) | 142.7(5) |
| | | Mn−$O_{phenolate}$(320) | 2.640 |
| | | Mn−$O_{phenolate}$(320)−Mn′ | 94.7 |

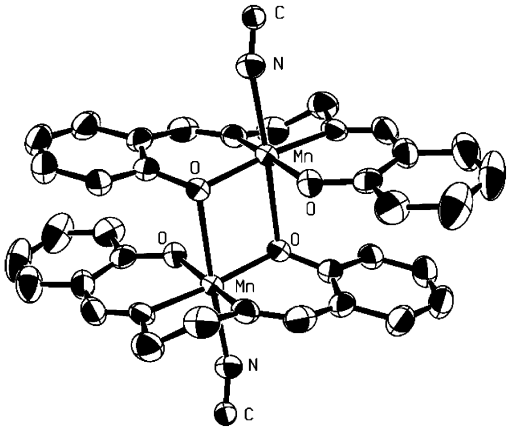


**Figure 4.** Dinuclear subunit [{Mn(NC)(salen)}($\mu$-O)$_2${Mn(NC)(salen)}] of the Mn1 or Mn3 center of **2**.

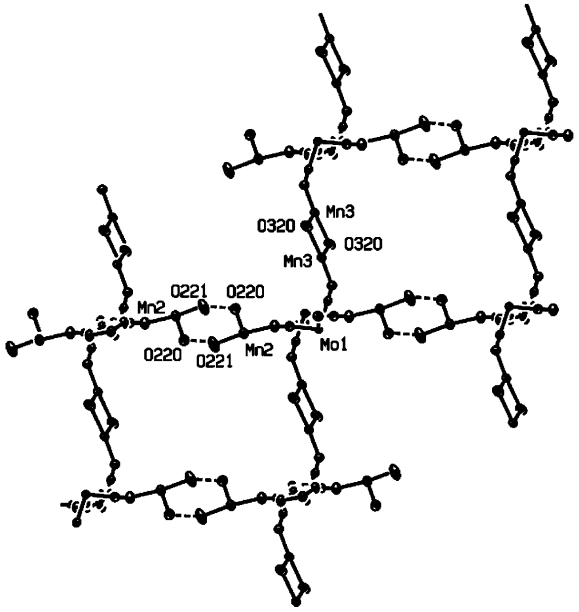


**Figure 5.** Hydrogen bonding and $\pi-\pi$ stacking interactions between chains in **2**.

teractions through the CN bridges lead eventually to the ground state with the total spin $S_T = {}^3/_2$.

Isothermal magnetization curves at $T = 1.9$ and 4.3 K in the applied field 0−50 kOe are shown in Figure 7. The curves for the increasing and decreasing fields are identical. The magnetization at 50 kOe reaches 4.5 and 3.4 $\mu_B$ at $T =$ 1.9 and 4.3 K, respectively, which are higher values than the expected saturation value of 3 $\mu_B$ for the molecule of **1** with the total spin $S_T = {}^3/_2$. This behavior implies that,

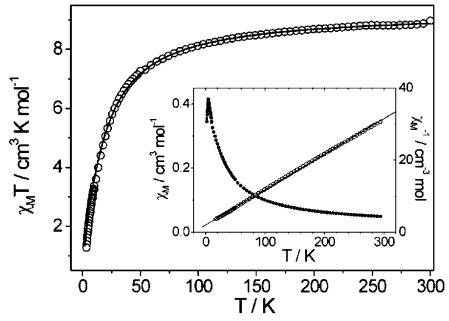


**Figure 6.** Thermal dependence of $\chi_M T$ vs $T$. Inset: $\chi_M$ vs $T$ (left scale) and $\chi_M^{-1}$ vs $T$ (right scale) for **1**.

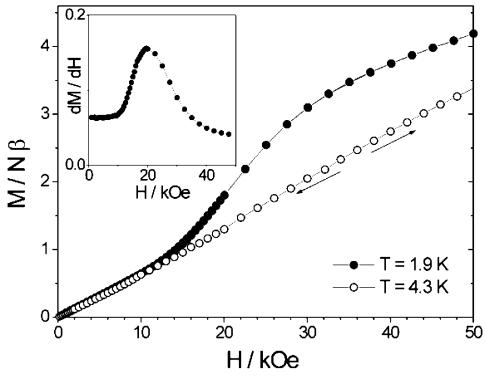


**Figure 7.** Field-dependent magnetization for **1** at $T = 1.9$ and 4.3 K.

besides the relative orientation of the tetrameric magnetic moments, the applied field influences the spin state of the molecule. In the higher field, the state with $S_T = {}^5/_2$ becomes occupied due to the small value of the intramolecular exchange integral ($J_1$).

The pronounced sigmoidal shape of the $M(H)$ dependence at $T = 1.9$ K shows the metamagnetic-like behavior characteristic for the systems in which the magnetocrystalline anisotropy is superimposed on the exchange couplings. Similar features have been recently observed for Cu(II)−W(V) coordination polymers with 2-D structures.[21] The shape of the $T = 1.9$ K curve suggests that the effective anisotropy field ($H_A$) is less than the exchange field ($H_E$), in contrast to the case of metamagnets, where $H_A \geq H_E$ and an immediate *spin−flip* transition to the saturated ferromagnetic state occurs. When the anisotropy field is of moderate intensity, the magnetization process proceeds through the *spin−flop*

(21) (a) Li, D.-F.; Zheng, L. M.; Wang, X. Y.; Huang, J.; Gao, S.; Tang, W. X. *Chem. Mater*. **2003**, *15*, 2094. (b) Ohkoshi, S.-I.; Arimoto, Y.; Hozumi, T.; Seino, H.; Mizobe, Y.; Hashimoto, K. *Chem. Commun.* **2003**, 2772.

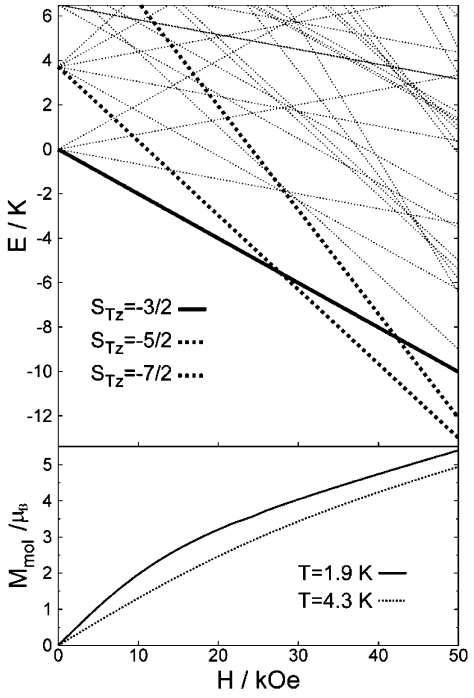


**Figure 8.** Top: Energy spectrum of an isolated tetrameric unit in an external magnetic field. The three lowest levels have been labeled. Bottom: Magnetization ($M_{mol}$) vs external magnetic field ($H$) calculated for the isolated molecule of **1**.

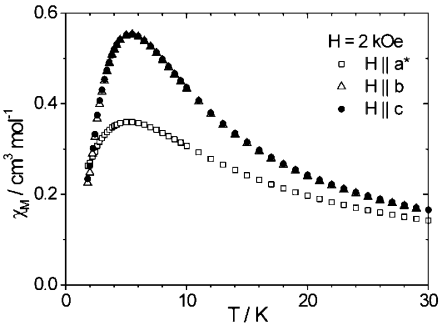


**Figure 9.** Thermal dependence of the magnetic susceptibility of a single crystal of **1**.

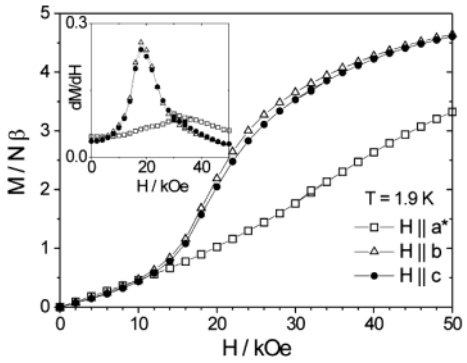


**Figure 10.** Field-dependent magnetization of a single crystal of **1** at $T$ = 1.9 K.

connected with reorientation of the antiferromagnetically coupled spins to the configuration perpendicular to the field. The threshold field for the *spin−flop* in the polycrystalline sample is 9 kOe, while the inflection point of the $M(H)$ curve (Figure 7, inset) occurs at $H_{SF}$ = 21 kOe. The effective anisotropy field ($H_A$) can be estimated from the $H_{SF}$ value using the simple relation $H_A = H_{SF}^2/2H_E$, where $H_E$ is the exchange field.[22] The magnetic moment of the $Mn^{III}_3W^V$ tetramer of 3 $\mu_B$ and the $T_N$ value 4.6 K gives the exchange field value $H_E \approx 23$ kOe, and the anisotropy field at $T$ = 1.9 K is then equal to $H_A \approx 19$ kOe. At $T$ = 4.3 K, the $M(H)$ curve hardly shows any transition, most probably due to the change of the $H_A/H_E$ ratio.

The energy spectrum of an isolated tetrameric $Mn^{III}_3W^V$ molecule in an external magnetic field provides the foundation of the *spin−flop* transition (Figure 8, top). The first intersection of the $S_{Tz} = -3/2$ level of the ground state multiplet with the $S_{Tz} = -5/2$ level of the multiplet of the first excited state occurs in the field of ~28 kOe. The latter remains the lowest one in the spectrum up to 50 kOe. This means that in the investigated range of magnetic fields the thermal average of the magnetization of an isolated tetrameric unit ($M_{mol}$) ($J' = 0$) will undergo a considerable change. The $M_{mol}$ versus $H$ curves calculated numerically (Figure 8, bottom) illustrate the above, attaining an average magnetization of 5.4 and 4.9 $\mu_B$ for $T$ = 1.9 and 4.3 K, respectively, at $H$ = 50 kOe.

**Single-Crystal Magnetic Measurements for 1.** For single-crystal magnetic measurements, a platelet single crystal having a size of 0.8 × 0.6 × 0.2 mm$^3$ was selected, and the orientation of the axes of the crystal was determined by X-ray analysis. The temperature dependence of magnetization was measured upon cooling in the temperature range 1.9−250 K for the external magnetic field 2 kOe applied in three perpendicular directions along the *a**, *b*, or *c* crystal axes. At 250 K, the susceptibilities along all three axes were the same, but upon cooling, they started gradually to separate. The $\chi_M$ versus $T$ plots in the range 1.9−30 K are shown in Figure 9, where external magnetic fields are applied in three perpendicular directions along the *a**, *b*, or *c* crystal axes. While the temperature is lowered, $\chi_M$ measured in the three directions increases smoothly, reaches its maximum value at about $T$ = 4.6 K, and then decreases abruptly, which does again reveal evidence of the long-range magnetic ordering below this temperature. The data corresponding to $H \| b$ and to $H \| c$ show a larger maximum value than the $H \| a^*$ data. This behavior suggests the existence of planar magnetic anisotropy in **1**, which is present in the system already above $T_N$. The susceptibility for $H \| b$ or $H \| c$ at $T = T_N$ decreases rapidly toward zero as the temperature is lowered, while that for $H \| a^*$ does not change much. Such behavior resembles a parallel susceptibility (the case for $H \| b$ or $H \| c$) or a perpendicular susceptibility (the case for $H \| a^*$) of an ordered uniaxial antiferromagnet. The coincidence of the results for $H \| b$ and for $H \| c$ implies that, instead of the easy axis, **1** displays the easy plane of magnetization. Such a planar type of anisotropy is probably due to the relation of $Mn^{III}_3W^V$ molecules by the inversion center in the crystal structure.

The field dependence of the magnetization at $T$ = 1.9 K is shown in Figure 10. The curves do not display any hysteresis effect. As for the polycrystalline sample, the $M(H)$

(22) deJongh, L. J.; Miedema, A. R. *Adv. Phys.* **1974**, *23*, 220.

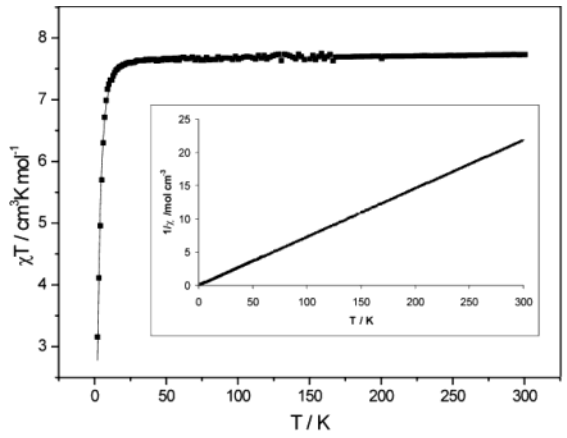


**Figure 11.** Thermal dependence of $\chi_M T$ vs $T$ of **2**·3.5$H_2O$. Inset: $\chi_M{}^{-1}$ vs $T$.

plots have a sigmoidal shape, clearly outlined for $H\|b$ or $H\|c$, and are strongly suppressed for the measurements in the $a^*$ direction. The shape of the curves and coincidence of the values for the $b$ and $c$ directions in contrast to that for the $a^*$ direction confirm the planar anisotropy in **1**. In the low-dimensional compounds it is often the case that the *spin−flop* transition is observed only in one direction, like in $[(CH_3)_3NH]FeCl_3 \cdot 2H_2O$ or $Ba_3Cu_2O_4Cl_2$.[23,24] It appears that the *spin−flop* transition for $H\|b$ or $H\|c$ takes place at $H_{SF} = 18$ kOe, while for $H\|a^*$ it occurs only at 30 kOe and is much weaker (Figure 10, inset). The distinct *spin−flop* transition observed for the *bc* plane and the temperature dependence of susceptibility below $T_N$ suggest that the spins of the molecules reside mainly in the *bc* plane or, at least, close to that plane.

**Magnetic Properties of 2·3.5$H_2O$.** Variable-temperature (2−300 K) magnetic susceptibility data were collected on a polycrystalline sample of **2**·3.5$H_2O$ in a field of 1 kOe (Figure 11). The room-temperature $\chi_M T$ value 7.75 $cm^3$ K $mol^{-1}$ (7.87 $\mu_B$) is significantly lower than the expected spin-only value (9.00 $cm^3$ K $mol^{-1}$, 8.48 $\mu_B$) for the three high-spin Mn(III) ions ($S = 2$, $g = 2.00$). The value of $\chi_M T$ remains relatively temperature independent in the 300−29 K range and then rapidly decreases to reach 3.16 $cm^3$ K $mol^{-1}$ (5.03 $\mu_B$) at 2 K. This sharp decrease and a negative Weiss constant of $\Theta = -0.40$ K (2−300 K) are indications of antiferromagnetic interactions between the Mn(III) centers. To estimate the coupling constant ($J_1$) between the Mn(III) centers in **2**·3.5$H_2O$, calculations based on the Hamiltonian $\mathbf{H} = -J_1 S_{Mn1} S_{Mn2}$ were performed. The following assumptions have been taken: (i) the identical magnetic interactions between two Mn(III) centers through the phenolate bridges, (ii) an isotropic Heisenberg coupling between manganese(III) centers through the diamagnetic $[Mo^{IV}(CN_8)]$ spacer in the cyano-bridged $\{Mn_3Mo\}_n^-$ repeating unit.[25−28] The $\chi_M T$ values have been theoretically simulated by using the Van Vleck formula, which demands the energies of the different spin levels to be expressed as a function of $J_1$.[29] To model these interactions, the $\chi_M T = \chi_{mer} T/[1 - \chi_{mer}(J_2/Ng^2\beta^2)]$ approximation has been applied, where $\chi_{mer}$ denotes the magnetic susceptibility of an isolated repeating unit and $J_2$ is the coupling constant between $Mn_3Mo$ repeating units. The best fit has been obtained with the coupling constant $J_1 = -0.81$ $cm^{-1}$, the coupling constant $J_2 = +0.04$ $cm^{-1}$, and the mean Landé factor $g = 2.27$. Taking into account both coupling constant values, the overall magnetic effect in **2**·3.5$H_2O$ is antiferromagnetic in character and very weak.

## Conclusions

The self-assembly reaction between $[Mn^{III}(salen)(H_2O)]^+$ and $[W^{IV}(CN)_8]^{4-}$ or $[Mo^{IV}(CN)_8]^{4-}$ leads to materials with different structures and various magnetic properties. While $[Mn^{III}(salen)H_2O]_3[W^V(CN)_8] \cdot H_2O$ (**1**) consists of magnetically bound tetrameric $Mn_3{}^{III}W^V$ molecules showing antiferromagnetic long-range ordering with planar anisotropy, $[Mn(salen)(H_2O)_2]_2\{[Mn(salen)(H_2O)][Mn(salen)]_2[Mo(CN)_8]\} \cdot 0.5ClO_4 \cdot 0.5OH \cdot 4.5H_2O$ (**2**) represents the set of weakly coupled double-phenolate-bridged $[Mn^{III}(salen)]_2$ subunits, between which magnetic interaction through the diamagnetic $[Mo^{IV}(CN)_8]^{4-}$ spacer is practically negligible.

The formation of **1** and **2** is controlled by the concerted action of the redox potential of the $[M(CN)_8]^{3/4-}$ couple, competition of the octacyanometalate moiety with solvent water molecules at the $Mn^{III}$ center, as well as the equilibrium between monomeric $[Mn^{III}(salen)H_2O]^+$ and dimeric $[Mn^{III}{}_2(salen)_2(H_2O)_2]^{2+}$ forms in aqueous solution.

Our results suggest the possibility of design and construction of single molecule magnets or high-spin molecules based on Schiff-base cationic precursors and octacyanometalates. Further work on the supramolecular systems along this line with Mn(III) salen analogues and related ligands is currently in progress.

**Acknowledgment.** We are grateful to Prof. Michel Verdaguer for fruitful discussions. This work was partially supported by the ESF (Molecular Magnets Program) and the State Committee for Scientific Research in Poland (KBN) Grant No. 2P03B 111 24.

**Supporting Information Available:** Figures showing the main intermolecular interactions in the crystalline network of compound **1**, the main interactions between the two chains in compound **2**, and the hydroxyl ion in the crystal lattice of compound **2** (with a detailed description), tables showing the selected bond distances and angles and the hydrogen bonds of compound **1**, and X-ray crystallographic files in CIF format for compounds **1** and **2**. This material is available free of charge via the Internet at http://pubs.acs.org.

IC035464N

(23) Greeney, R. E.; Landee, C. P.; Zhang, J. H.; Reiff, W. M. *Phys. Rev. B* **1989**, *39*, 12200.
(24) Wolf, M.; Ruck, K.; Eckert, D.; Krabbes, G.; Müller, K.-H. *J. Magn. Magn. Mater.* **1999**, *196−197*, 569.
(25) Bonadies, J. A.; Kirk, M. L.; Soo Lah, M.; Kessissoglou, D. P.; Hatfield, W. E.; Pecoraro, V. L. *Inorg. Chem.* **1989**, *28*, 2037.
(26) Matsumoto, N.; Zhong, Z. J.; Okawa, H.; Kida, S. *Inorg. Chim. Acta* **1989**, *160*, 153.
(27) Mikuriya, M.; Yamato, Y.; Tokii, T. *Bull. Chem. Soc. Jpn.* **1992**, *65*, 1466.
(28) Clérac, R.; Miyasaka, H.; Yamashita, M.; Coulon, C. *J. Am. Chem. Soc.* **2002**, *124*, 12837.
(29) Kahn, O. *Molecular Magnetism*; VCH: New York, 1993; p 113.